Supporting Information for:

A Bio-Inspired, Small Molecule Electron-Coupled-Proton Buffer for Decoupling the Half Reactions of Electrolytic Water Splitting

Benjamin Rausch, Mark D. Symes, and Leroy Cronin*

WestCHEM, School of Chemistry, The University of Glasgow, University Avenue, Glasgow, G12 8QQ, UK.

E-mail:lee.cronin@glasgow.ac.uk
http://www.croninlab.com

Index *Page*

SI-1: General Experimental Remarks: All solvents were purchased from Sigma Aldrich. 0.180 mm-thick Nafion N-118 membrane and carbon felt were purchased from Alfa Aesar. All chemical reagents and solvents were used as purchased, except for sodium hydroquinone sulfonate, which was either purchased from Tokyo Chemical Industries and recrystallized from hot DI water or purchased from Sigma, washed with ethanol and then recrystallized from hot DI water. All electrolyte solutions were prepared with reagent grade water (18 MΩ-cm resistivity). pH determinations were made with a Hanna HI 9124 waterproof pH meter. UV/vis measurements were performed on a 100 TIDAS spectrophotometer using 10 mm optical path quartz cuvettes or with an external Hellma Analytics fibre optic probe (661.302-UVS, Ganz-Quartz Tauchsonde, 5 mm, SN-Nr. 10143).

SI-2: Electrochemical methods: Three-electrode electrochemical studies were performed using a CH Instruments CHI760D. Unless stated otherwise, three-electrode electrochemistry was performed using a 3 mm diameter glassy carbon disc working electrode (Princeton Applied Research) with a large area Pt mesh counter electrode and an Ag/AgCl reference electrode (BASi) at room temperature and pressure, under ambient atmospheric conditions. Solutions for cyclic voltammetry were quiescent, whilst both compartments of the H-cells were stirred during bulk electrolyses. Stirred three-electrode current-potential curves were performed using a 2 mm diameter Pt disc working electrode (Princeton Applied Research) or a 3 mm diameter glassy carbon working electrode (Princeton Applied Research) with a large area Pt mesh counter electrode and an Ag/AgCl reference electrode (BASi) at room temperature and pressure, under ambient atmospheric conditions, with *i*R compensation enabled. Currents were measured after a period of 2 minutes at a given potential, and all data points were obtained three times and averaged. Potentials were converted to NHE potentials by using E(NHE) = E(Ag/AgCl) +0.197 V. Two-electrode experiments were performed using a CH Instruments CHI760D potentiostat by attaching the counter and reference leads to the same electrode, thus giving a floating reference configuration. The compartments of the H-cells were separated by a piece of 0.180 mm-thick Nafion membrane, with this membrane being held in place by judicious application of Araldite epoxy glue (Bostik Findley, Ltd., UK). The applied voltages were corrected for the ohmic resistance of the cells (the *i*R drop), to give an effective voltage ($V_{effective}$) for the potential-current curves according to the formula:[S1]

$$V_{effective} = V_{applied} - iR$$

where *i* is the current flowing through the cell and R is the resistance of the cell. Cell resistances were measured by the *i*R test function available on the potentiostats. The error associated with these *i*R-corrected curves is dominated by the error associated with gauging the resistance of the solution, where values were found to vary over a range of $R_{measured}$ ±3%.

SI-3: Cycling from ECPB* to ECPB and back to ECPB*: After oxidation to the benzoquinone sulfonate ($C_6H_3SO_5^-$), the ECPB could be re-reduced to the hydroquinone sulfonate (ECPB*, $C_6H_5SO_5^-$) in either a two-electrode or a three electrode configuration by applying potentials cathodic of the redox wave in the CV in Figure 1 (see main text). Considering first the oxidation of ECPB*, as this proceeded at the working electrode, bubbles of hydrogen were visible at the counter electrode and upon complete oxidation of ECPB* the solution had changed to a dark orange color, the pH was only partly changed (see section SI-8) and H_2 production at the

counter electrode ceased. Examples of multiple consecutive and complete reduction/oxidation cycles of the ECPB are given in Figures S2 – S10. These experiments were performed numerous times, in both three- and two-electrode configurations, using different electrodes, ECPB concentrations, in both H_3PO_4 and additional supporting electrolytes (NaCl, Na_2HPO_4, NaH_2PO_4) and at different pH ranges (0.7 to 8.7). A typical reaction was as follows: 20 mL of a colorless 20 mM solution of $C_6H_5SO_5^-$ in 1.8 M H_3PO_4 (pH 0.7) was taken in one compartment of an H-cell. This chamber was further equipped with a large area carbon felt counter electrode; the reference electrode was clipped to the same electrode for a two electrode set-up. The other compartment of the H-cell was filled with 25 mL of 1.8 M H_3PO_4 (pH = 0.7) and equipped with a Pt mesh "working electrode". The compartments of the cell were separated by a Nafion membrane. Electrolysis was initiated at −0.8 V with respect to the working electrode at room temperature (reducing protons at the working electrode and oxidising the ECPB* at the carbon counter electrode) and open to air without degassing, and the hydroquinone was observed to turn orange. Bubbles were visible at the working electrode. Electrolysis was stopped after –75.4 C had been passed. The oxidized sample was then re-reduced at a potential of +1.8 V on the working electrode in a two-electrode configuration as before, and +75.1 C of charge was extracted, equating to 99.6% of the charge originally stored in the oxidized ECPB. Three completed oxidation-reduction cycles for this sample are given in Figures S2 – S4. After the first such cycle, the reduced ECPB* returned to its original colorless state, and a UV/vis spectrum of this solution was found to match to within 7% the spectrum of a fresh solution of $C_6H_5SO_5^-$ in H_3PO_4 at the same concentration (Figure S17).

SI-4: Gas Chromatography: Gas chromatography headspace analysis (GCHA, Figures 3b and 4b in the main text) was conducted in airtight H-cells in a two-electrode configuration, using an Agilent Technologies 7890A GC system by direct injection of gas using a gas-tight syringe. The protocol for the electrochemistry required for these analyses is given in section SI-5. The column used was a 30 metre-long 0.320 mm widebore HP-molesieve column (Agilent). The GC oven temperature was set to 27 ºC and the carrier gas was Ar. The front inlet was set to 100 °C. The GC system was calibrated for O_2 and H_2 using certified standards of these gases at a range of volume % in argon supplied by CK Gas Products Limited (UK). Linear fits of volume % *vs.* peak area were obtained, which allowed peak areas to be converted into volume % of O_2 and H_2 in the H-cell headspace. A small air leak into the cell introduced during sampling was corrected for by calibrating the amount of O_2 and N_2 in air and then applying appropriate corrections for these based on the amount of N_2 observed in the chromatographs. Total H-cell/GC system headspaces were calculated by filling the cells with water at room temperature. Typical headspaces were on the order of 107 mL. ECPB reduction at one electrode and water oxidation at the other gave oxygen (but no hydrogen was detected in the headspace). Similarly, ECPB* oxidation at one electrode and reduction of protons at the other gave hydrogen and essentially no oxygen (*vide infra*) within the detection limits of the GC system, which were gauged to be ±0.04% H_2 in the headspace and ±0.08% O_2 in the headspace. Charges passed were converted into expected volume % of hydrogen in the headspace by converting charges to an expected number of moles of H_2 (by dividing by 2*F*, where *F* is the Faraday constant), and then taking the volume of 1 mole of an ideal gas at standard temperature and pressure to be 22.4 L. Faradaic efficiencies were then calculated by taking the ratio of gas volume % based on the charge passed to the gas volume % measured by GC. All H_2 determinations were performed at least five times, and average Faradaic efficiencies were 98% (±7%) for a Pt working electrode (performing the HER) in combination

with a carbon counter electrode (oxidising ECPB*) in a two-electrode set-up. The amount of oxygen in each measurement was corrected for air leaks by comparison with the amount of nitrogen in each sample. After passing 50 Coulombs of charge for ECPB* oxidation, only a trace of the O_2 observed in the chromatograph could not be accounted for by considering the air leak, with this "excess" oxygen equating to < 2% of the amount of O_2 which would be expected if the HER and OER were occurring concurrently. The real amount of O_2 not emanating from the air leak may indeed have been smaller than even this lower bound; however, a slight overlapping of the peaks for hydrogen and oxygen in the chromatogram means that <2% is a more accurate description of the data. The single biggest source of error was the estimation of the cell headspace (±1 mL).
For oxygen production, charges passed were converted into expected volume % in the headspace by converting charges to an expected number of moles of O_2 (by dividing by 4*F*, where *F* is the Faraday constant), and then taking the volume of 1 mole of an ideal gas at standard temperature and pressure to be 22.4 L. Faradaic efficiencies were then calculated by taking the ratio of gas volume % based on the charge passed to the gas volume % measured by GC. O_2 determinations were performed at least three times, and average Faradaic efficiencies were 91% (±5%) for a Pt working electrode (performing the OER) in combination with a carbon counter electrode (reducing ECPB) in a two-electrode set-up.

SI-5: OER and HER at a Pt electrode with a concentrated ECPB solution: The working electrode chamber of a two compartment H-cell was charged with 1.8 M H_3PO_4 (pH = 0.7), whilst the counter electrode chamber was filled with a 50:50 mix of 0.5 M $C_6H_5SO_5^-$ and its corresponding oxidized form $C_6H_3SO_5^-$ in 1.8 M H_3PO_4, at pH 0.7. The working electrode was a 0.031 cm^2 area platinum disc electrode and the combined counter/reference electrode (two-electrode configuration) was a large area carbon felt. The two chambers of the H-cell were separated by a Nafion membrane, so that cations (H^+ and K^+) could travel freely between compartments, but the movement of anions was attenuated.

Figures 3a and 4a in the main text show how the current density through such a two-electrode cell varies with the magnitude of the effective applied voltage (as set on the Pt electrode in the 1.8 M H_3PO_4). Also shown for comparison are the current density curves for the same cell set-up, but where both chambers were filled with 1.8 M H_3PO_4 (*i.e.* using no ECPB), both with a large area carbon counter/reference electrode and where the carbon felt was replaced by a platinum mesh counter/reference electrode to avoid any oxidative degradation of the carbon. From Figures 3a and Figure 4a in the main text, it is apparent that much greater current densities are obtained at a given voltage when the ECPB is used, whether the voltage applied is positive (oxidation of water at the nominal working electrode, Figure 4a) or negative (reduction of protons at the working electrode, Figure 3a). In support of this, steady bubbling from the "working" electrode was observed when the counter electrode compartment was filled with ECPB/ECPB* and effective voltages of greater magnitude than +1.6 V, or −0.7 were applied to the working electrode (Figures 3a and 4a in the main text). No bubbling was visible from either electrode until voltages of at least ±2 V were used in cells using only 1.8 M H_3PO_4 and using two Pt electrodes, as expected from Figures 3a and 4a. Gas chromatography headspace analysis (GCHA) was used to confirm the nature and amount of the gases evolved under these conditions (see above).

SI-6: Electrochemical system efficiency: A 0.5 M solution of hydroquinone sulfonate in 1.8 M H_3PO_4 (pH 0.7) was oxidized until a 50:50 mix of the oxidized and two electron-reduced states had been produced. This 50:50 mix (ECPB/ECPB*) was then used to test the efficacy of hydroquinone sulfonate as an ECPB. ECPB-based measurements were taken in a three-electrode set-up, using a glassy carbon working electrode and were compared to a platinum working electrode in an ECPB-free solution at the same pH.

As the Faradaic efficiency for both oxygen evolution and hydrogen evolution are essentially 1, we can compare the overall system efficiency for electrochemically-driven water splitting on Pt and carbon electrodes by comparing the voltages required to deliver certain current densities.

Taking a benchmark current density of 50 $mAcm^{-2}$, Figure 2a (main text) shows that reduction of ECPB to ECPB* on glassy carbon will proceed at 50 $mAcm^{-2}$ when a bias of +0.23 V (*vs.* NHE) is applied, whilst −0.39 V is required to reduce protons to hydrogen on Pt at this current density. Conversely, Figure 2b (main text) shows that oxidation of ECPB* at 50 $mAcm^{-2}$ on glassy carbon proceeds at +0.90 V, whereas oxidation of water on Pt at 50 $mAcm^{-2}$ requires +2.23 V. Given that the use of a three-electrode configuration should minimize the effects of resistance on these metrics,[S1] it is possible to quantify the expected energetics of a two-step ECPB system (using a glassy carbon electrode to oxidize and reduce the ECPB and a Pt electrode to alternately oxidize water and reduce protons) versus a single step system that uses two Pt electrodes to produce O_2 and H_2 simultaneously. Hence, to oxidize water and reduce the ECPB at 50 $mAcm^{-2}$ requires (2.23 – 0.23 =) 2.00 V, with the reverse step (re-oxidation of ECPB* and simultaneous proton reduction to H_2) needing (+0.9 − −0.39 =) 1.29 V. This gives an overall voltage requirement of 3.29 V for the two step process compared to 2.62 V (+2.23 − −0.39) for the single step reaction. This gives an expected efficiency of 80% for the two step process that uses a single Pt electrode relative to the single step process (using 2 Pt electrodes) in the absence of resistive factors.

SI-7: UV/vis studies to determine the rate at which the quinone to crosses the Nafion membrane: A 0.5 M solution of hydroquinone sulfonate in 1.8 M H_3PO_4 (pH 0.7) was placed in one compartment of an H-cell. The second compartment was filled with 1.8 M H_3PO_4 (pH 0.7) and an external fibre optic UV/vis probe was placed in this compartment. Both compartments were stirred and kept in the dark under air. UV/vis spectra were recorded every 60 minutes for 72 hours. For the calibration of the crossing rate, UV/vis spectra of several concentrations of hydroquinone in 1.8 M H_3PO_4 (pH 0.7) were recorded and compared to the time-dependent UV/vis spectra (see Figure S16). The rate of crossing was thus determined to be 2.7 x 10^{-6} mol h^{-1}.

SI-8: pH buffering during water splitting with 1,4-hydroquinone sulfonate: In a representative experiment, 4 mL of a 0.5 M solution of hydroquinone sulfonate in 0.1 M HNO_3 (pH 0.70) was placed in one compartment of an H-cell along with a large surface area carbon electrode. The second compartment was filled with 7 mL of a 0.1 M HNO_3 solution (pH 0.63) and equipped with a large surface area platinum electrode. The two compartments were separated by a Nafion membrane. The platinum was connected as the working electrode, while the carbon felt was connected as the counter/reference electrode in a two-electrode set-up. The pH was recorded after it reached stability. The potential on the working electrode was set to −1.6 V and −206.11 C of charge was passed, driving the HER at the Pt electrode and oxidising hydroquinone sulfonate at the carbon electrode. This amount of charge would be expected to consume a total of 2.136 × 10^{-3} moles of protons from

the system, which are lost as evolved H_2. This in turn could be expected to impact on the measured pH in the two compartments in a number of ways. Three scenarios were considered, as detailed below (see also Table S1). In scenario 1, all the protons are taken from the compartment containing just the HNO_3 (*i.e.* the compartment in which the HER was occurring). This leaves the pH in the hydroquinone sulfonate compartment unchanged (0.70), but should give a new pH in the working electrode compartment of 12.85 (hence in this case, some reduction of water to give OH^- would also occur, and indeed such large pH changes using non-buffering ECPB candidates were seen in our previous study[S2]). In scenario 2, the protons are taken equally from both compartments, such that any initial imbalance between proton concentrations is maintained (that is to say, on average for each molecule of hydrogen that is produced, one proton is taken from the nitric acid compartment and one proton is taken from the ECPB compartment). This would cause a rise in the HNO_3 compartment pH from 0.63 to 1.09, and a much larger rise in the hydroquinone sulfonate compartment (0.70 to 12.83). Finally in scenario 3, protons are again taken from both compartments, but this time the pH of these compartments becomes the same. The resulting global pH is then calculated to be 1.56 in both compartments after the stated amount of charge is passed.

Table S1. Comparison of observed and potential pH values of the HNO_3 (7 mL) and the ECPB (4 mL) compartments in a typical electrolysis experiment in the absence of a buffered solution.

	HNO_3 compartment	ECPB compartment
Initial pH	0.63	0.70
Scenario 1	12.85	0.70
Scenario 2	1.09	12.83
Scenario 3	1.56	1.56
Measured after passing −206.11 C	0.75	0.48

In the event, after −206.11 C of charge was passed, the pH in the HNO_3-only compartment had risen only to 0.75 (from an initial 0.63), whilst the pH in the hydroquinone sulfonate compartment had fallen from 0.70 to 0.48. Overall, the number of moles of H^+ in the system as a whole therefore *increased* by 1.3×10^{-4} moles during the hydrogen evolution step. From Figures S13, S14 and S17, a degradation of ~5% could be expected for the oxidized form of the ECPB over the time course of this electrolysis (6 hours). This equates to a loss in oxidized ECPB of $\sim 1 \times 10^{-4}$ moles. The expected degradation pathway for the oxidized ECPB is *via* dimerisation and oligomerisation, with the release of protons (one per quinone derivative for dimerization).[S3] Hence we suggest that this decrease in pH can be largely accounted for by the degradation of the oxidized ECPB. This in turn we interpret as evidence that those molecules of the ECPB that do not oligomerize are acting to buffer the pH of the solution to a certain extent, as we do not measure the large pH rises that would be expected were no buffering occurring at all. This experiment was repeated several times in both two- and three-electrode set-ups, with comparable results obtained each time.

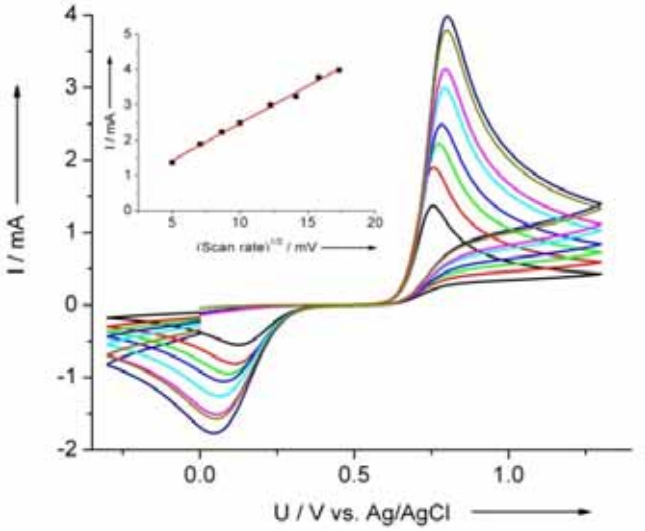

Figure S1. CVs of 25 mM ECPB/ECPB* at various scan rates. The supporting electrolyte was 1.8 M H_3PO_4 (pH 0.7). A three-electrode, single-compartment set-up was used, with a glassy carbon working electrode (area = 0.071 cm^2), platinum mesh counter electrode and an Ag/AgCl reference electrode. The scan rates used were: 25 mVs^{-1} (black), 50 mVs^{-1} (red), 75 mVs^{-1} (green), 100 mVs^{-1} (dark blue), 150 mVs^{-1} (light blue), 200 mVs^{-1} (magenta), 250 mVs^{-1} (khaki), 300 mVs^{-1} (navy blue). The inset shows a graph of the peak current versus square root of the scan rate for the oxidation event associated with the anodic wave over the scan-rate range of 25-300 mVs^{-1}. The linear fit is provided as a guide to the eye. The error associated with the measurement of the current was ±0.1 mA on each reading, which corresponds to the size of the data markers in the inset. All experiments were performed without degassing and under air.

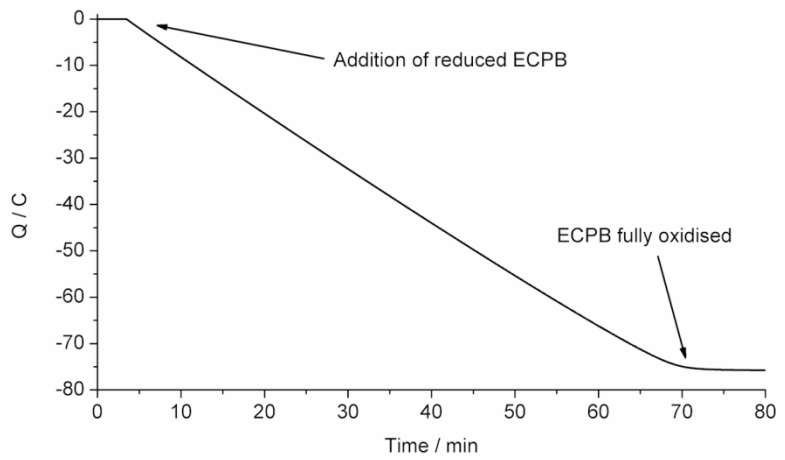

Figure S2. Controlled bulk electrolysis in a 2-electrode, 2-compartment set-up of 1.8 M H_3PO_4 (pH 0.7). The two chambers are separated by a Nafion 118 membrane. A large surface Pt mesh was used as the "working electrode" and a carbon felt as counter/reference electrode. The potential on the working electrode was poised at −0.8 V. Only a very small background current was observed, until 89 mg of potassium hydroquinone sulfonate (to give a 20 mM solution of hydroquinone sulfonate) was added to the compartment with the carbon electrode. The current increased by a factor of 78 until all the hydroquinone sulfonate had been oxidized, after which the current fell off to around its initial value.

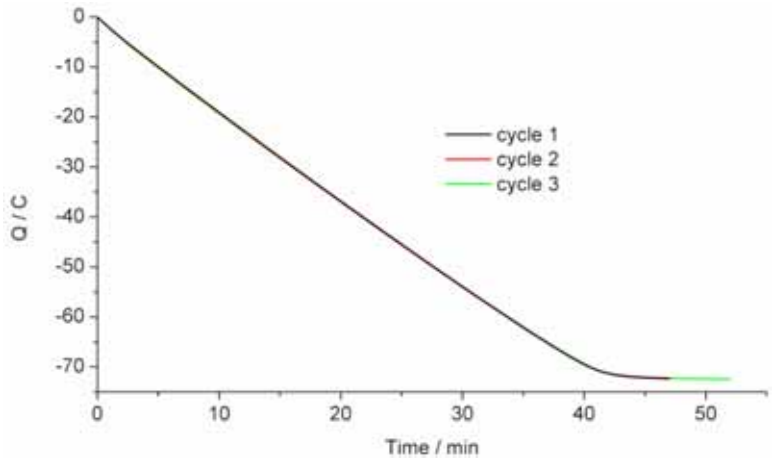

Figure S3. Controlled bulk electrolysis in a 2-electrode, 2-compartment set-up, with a large area Pt mesh "working electrode" and a carbon felt as counter/reference electrode. 18 mL of a 20 mM hydroquinone sulfonate solution in 1.8 M H_3PO_4 (pH 0.7) was placed in the counter electrode compartment and the working electrode compartment was filled with 1.8 M H_3PO_4. The compartments were separated by a Nafion 118 membrane. The working electrode was poised at −1.2 V (reducing protons, with concomitant oxidation of hydroquinone sulfonate at the carbon counter electrode). Three oxidation cycles of the initially fully reduced hydroquinone sulfonate solution are shown. The corresponding reduction graphs are shown in Figure S4.

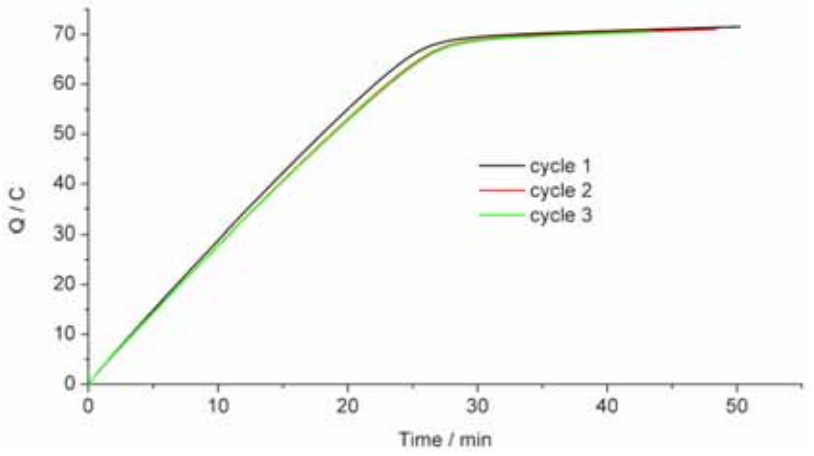

Figure S4. Controlled bulk electrolysis in a 2-electrode, 2-compartment set-up, with a large area Pt mesh "working electrode" and a carbon felt as counter/reference electrode. 18 mL of a 20 mM hydroquinone sulfonate solution in 1.8 M H_3PO_4 (pH 0.7) was placed in the counter electrode compartment and the working electrode compartment was filled with 1.8 M H_3PO_4. The compartments were separated by a Nafion 118 membrane. The working electrode was poised at +1.8 V (oxidizing water, with concomitant reduction of the benzoquinone sulfonate at the carbon counter electrode). Three reduction cycles are shown, corresponding to the oxidation graphs shown in Figure S3.

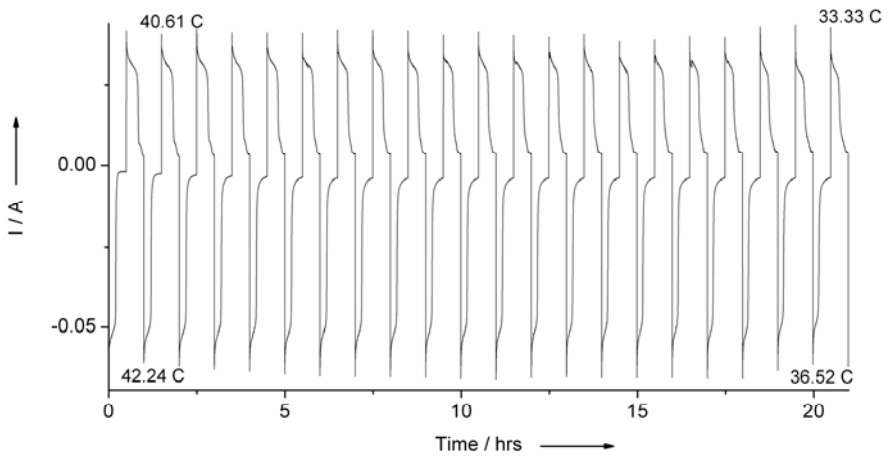

Figure S5. Multi potential step bulk electrolysis of a 10 mM hydroquinone sulfonate solution in 1.8 M H_3PO_4 (pH 0.7), in the counter electrode compartment of a 2-electrode, 2-compartment H-cell. A Pt mesh "working electrode" (in 1.8 M H_3PO_4 pH 0.7), and a carbon felt counter/reference electrode (in the hydroquinone sulfonate solution) were used, with the two compartments being separated by a Nafion 118 membrane. Voltages alternated between -1.2 V and +2.0 V on the Pt working electrode, alternately oxidizing and reducing the ECPB in the counter electrode compartment. 21 full cycles (starting with an oxidation of the hydroquinone in solution) are shown. The same set of data is used in Figures S13 and S14.

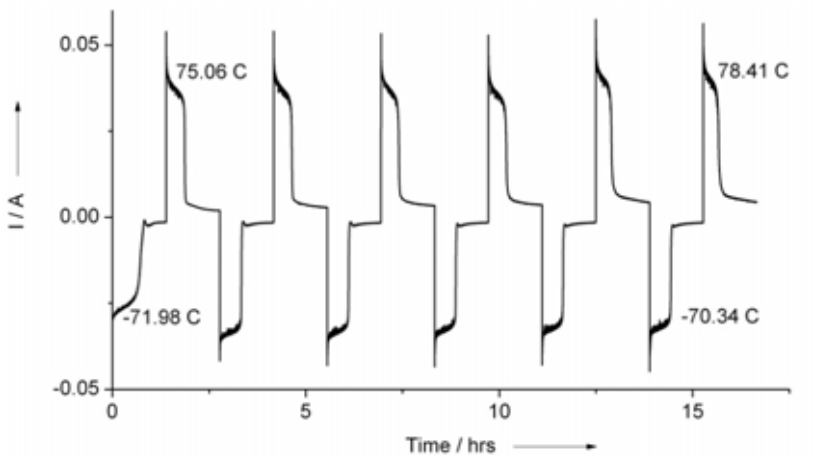

Figure S6. Multi potential step bulk electrolysis of a 20 mM hydroquinone sulfonate solution in 1.8 M H_3PO_4 (pH 0.7), in the counter electrode compartment of a 2-electrode, 2-compartment H-cell. A Pt mesh working electrode (in 1.8 M H_3PO_4 pH 0.7), and a carbon felt counter/reference electrode (in the hydroquinone sulfonate solution) were used, with the two compartments being separated by a Nafion 118 membrane. Voltages alternated between -1.2 V and +2.0 V on the Pt working electrode, alternately oxidizing and reducing the ECPB in the counter electrode compartment. 6 full cycles (starting with an oxidation of the hydroquinone in solution) are shown. The same sample was used in Figure S7 after 24h storage in the reduced form under bench-top conditions (exposed to air and light), giving an additional 5 cycles.

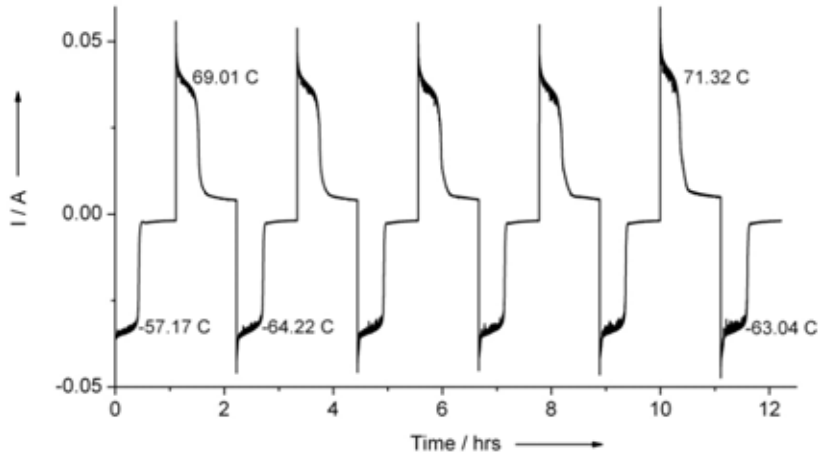

Figure S7. Multi potential step bulk electrolysis of a 20 mM hydroquinone sulfonate solution in 1.8 M H_3PO_4 (pH 0.7), in the counter electrode compartment of a 2-electrode, 2-compartment H-cell. A Pt mesh working electrode (in 1.8 M H_3PO_4 pH 0.7), and a carbon felt counter/reference electrode (in the hydroquinone sulfonate solution) were used, with the two compartments being separated by a Nafion 118 membrane. Voltages alternated between -1.2 V and +2.0 V on the Pt working electrode, alternately oxidizing and reducing the ECPB in the counter electrode compartment. 5.5 cycles are shown of the same sample as in Figure S6 after 24h storage in the reduced form under bench-top conditions (exposed to air and light). The difference between the first and the second hydroquinone sulfonate oxidations in Figure S7 suggests that there has been some light / air induced oxidation of the hydroquinone in solution. By comparison with the results shown in Figure S15, this suggests that the reduced quinone must be kept in the dark to avoid such spontaneous oxidation. Overall the capacity was decreased by 12% for the oxidation of hydroquinone sulfonate (compared to Figure S6) over 11 cycles over 2 days, while the benzoquinone sulfonate reduction capacity decreased by only 5% over the same time/number of cycles.

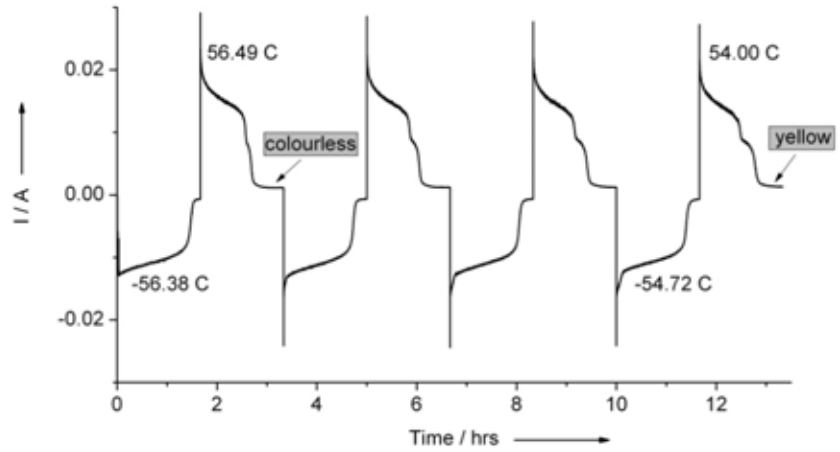

Figure S8. Multi potential step bulk electrolysis of a 20 mM hydroquinone sulfonate solution in phosphate buffer solution (0.5 M Na_2HPO_4, acidified to pH 4.20 using H_3PO_4) in the counter electrode compartment of a 2-electrode, 2-compartment H-cell. A Pt mesh working electrode (in 0.5 M Na_2HPO_4, acidified to pH 4.20 using H_3PO_4), and a carbon felt counter/reference electrode (in the hydroquinone sulfonate solution) were used, with the two compartments being separated by a Nafion 118 membrane. Voltages alternated between -1.2 V and +2.0 V on the Pt working electrode, alternately oxidizing and reducing the ECPB in the counter electrode compartment. 4 full cycles are shown. The capacity of the solution decreased by only by 3% for the hydroquinone sulfonate oxidation after 4 cycles and 4% for the benzoquinone sulfonate reduction respectively, but a second species/electrochemical process appears to be growing in that seems to be irreversible and turns the colorless reduced hydroquinone solution yellow.

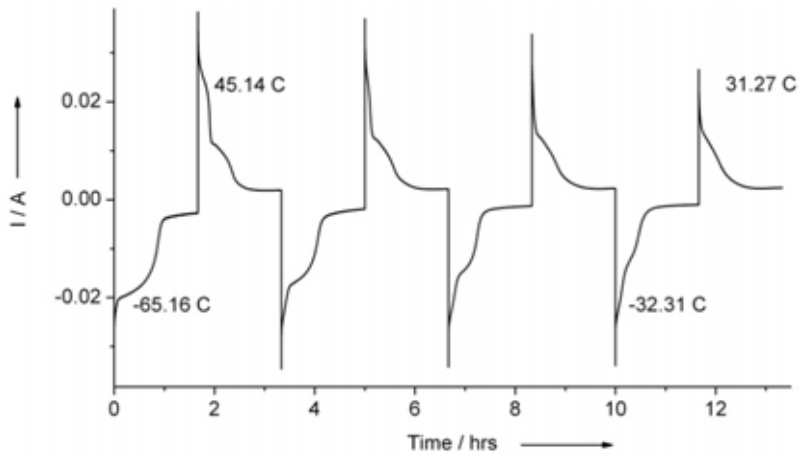

Figure S9. Multi potential step bulk electrolysis of a 20 mM hydroquinone sulfonate solution in phosphate buffer solution (0.5 M Na_2HPO_4, acidified to pH 7.01 using H_3PO_4) in the counter electrode compartment of a 2-electrode, 2-compartment H-cell. A Pt mesh working electrode (in 0.5 M Na_2HPO_4, acidified to pH 7.01 using H_3PO_4), and a carbon felt counter/reference electrode (in the hydroquinone sulfonate solution) were used, with the two compartments being separated by a Nafion 118 membrane. Voltages alternated between -1.2 V and +2.0 V on the Pt working electrode, alternately oxidizing and reducing the ECPB in the counter electrode compartment. 4 full cycles are shown. The capacity of the solution decreased by 50% for the hydroquinone sulfonate oxidation after 4 cycles and 31% for the benzoquinone sulfonate reduction respectively. These results are in line with the trend of oxidation/reduction of the ECPB being more irreversible at more basic pHs.

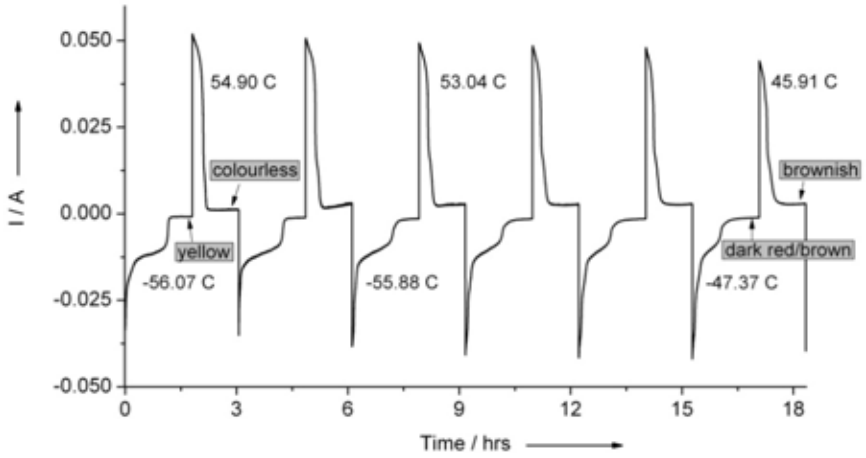

Figure S10. Multi potential step bulk electrolysis of a 20 mM hydroquinone sulfonate solution in 3.0 M NaCl solution (pH 8.4) in the counter electrode compartment of a 2-electrode, 2-compartment H-cell. A Pt mesh working electrode (in 1.0 M Na_3PO_4, acidified to pH 8.4 using H_3PO_4), and a carbon felt counter/reference electrode (in the hydroquinone sulfonate solution) were used, with the two compartments being separated by a Nafion 118 membrane. Voltages alternated between -1.8 V and +1.8 V on the Pt working electrode, alternately oxidizing and reducing the ECPB in the counter electrode compartment. 6 full cycles are shown. The oxidation/reduction capacity of the solution decreased by 16% after these 6 cycles.

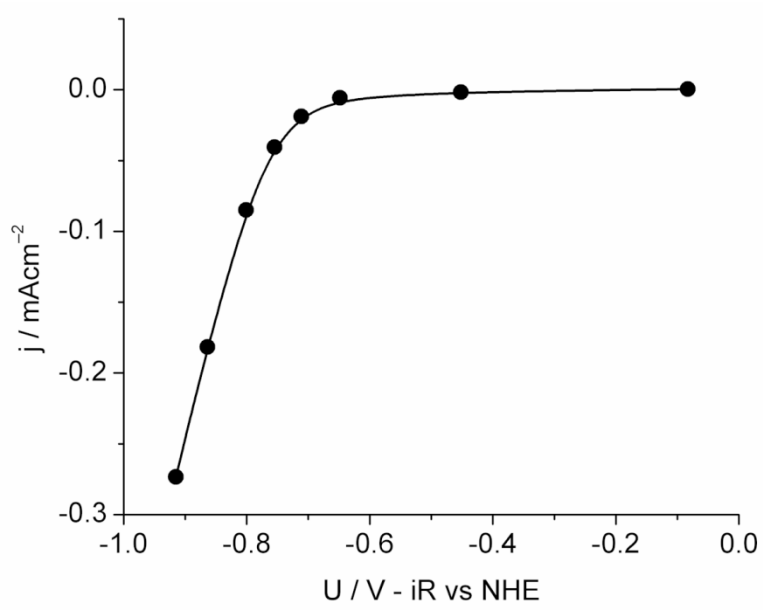

Figure S11. Three-electrode *i*-V curves in a stirred one-compartment, three-electrode set-up with an Ag/AgCl reference electrode and a large area Pt mesh counter electrode. The electrolyte was 1.8 M H_3PO_4 (pH 0.7) and the working electrode was a glassy carbon disc (area = 0.071 cm^2). The data shown is compensated for solution *i*R. A current density of 50 $mAcm^{-2}$ for hydrogen production was achieved at a voltage of −0.77 V *vs.* NHE.

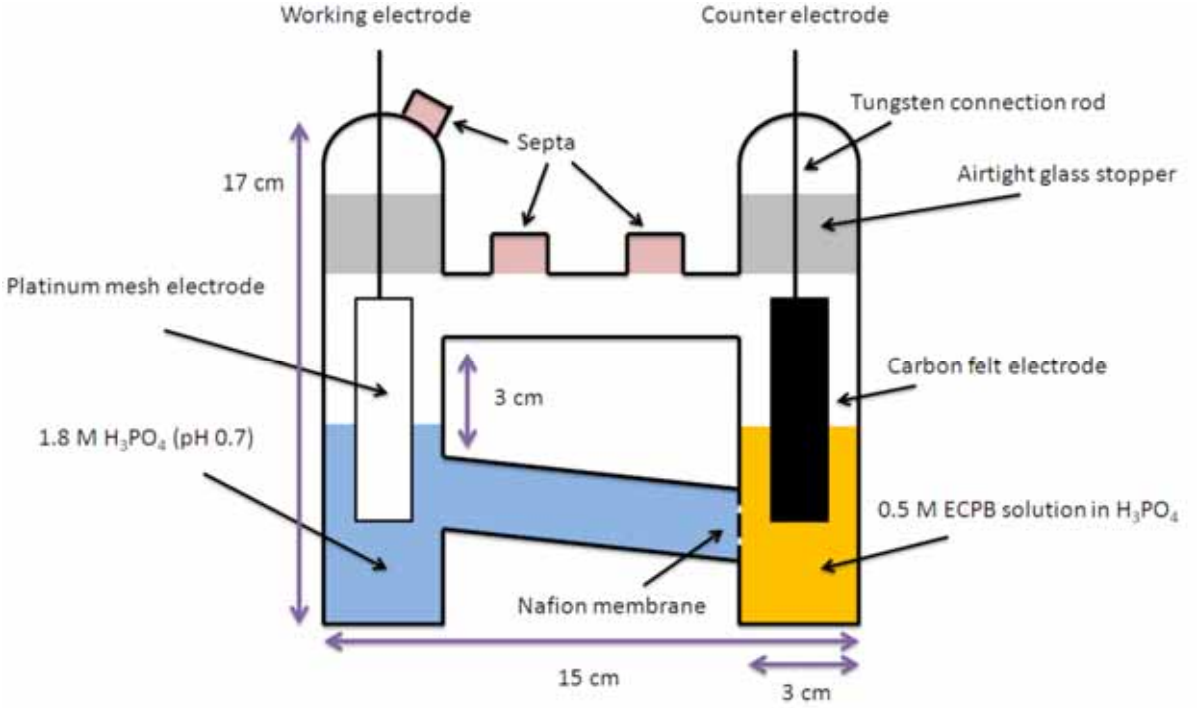

Figure S12. Schematic of the airtight H-cells used for gas chromatography. The dimensions are provided solely to give an approximate idea of the size of the cells, and varied between individual H-cells. Electrode ports were quick-fit glassware joints with rubber seals and screw tops. These were greased before reaction initiation. Both compartments were stirred during operation.

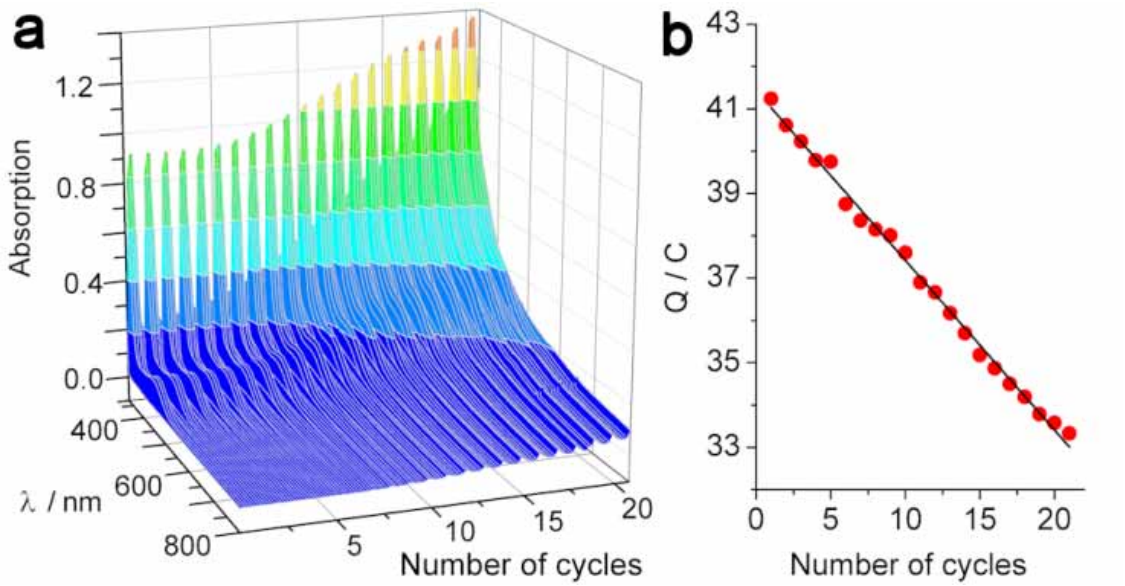

Figure S13a. Multiple UV/Vis spectra obtained at 10 minute intervals during the electrochemical cycling of a 10 mM sample of the ECPB in H_3PO_4 (1.8 M, pH 0.7), recorded using an external fibre optic probe. λ_{max} for the reduced species grows in at 362 nm and λ_{max} for the oxidized form is at 443 nm. 2D data from this graph are shown in Figure S14. **b:** Total charge passed during the full reduction of a 10 mM hydroquinone sulfonate solution in 1.8 M H_3PO_4 (pH 0.7) over 21 cycles.

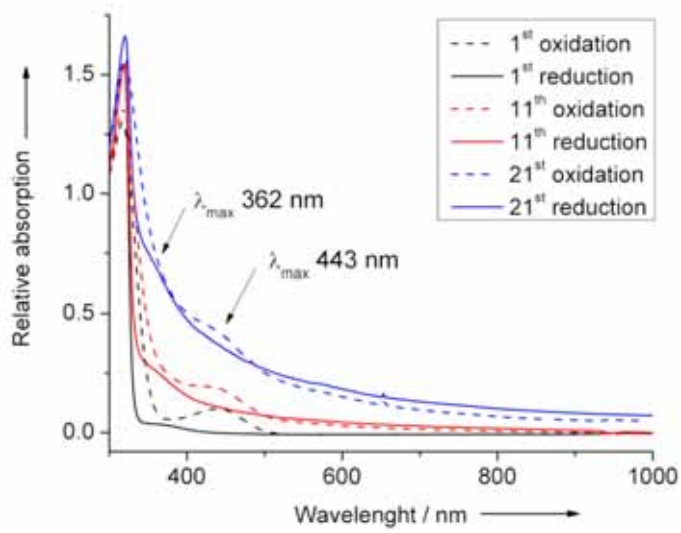

Figure S14. A comparison of the 2D UV-vis spectra (from Figure S13a) for the 1st, 11th and 21st full oxidation/reduction cycles of a 10 mM solution of hydroquinone sulfonate in 1.8 M H_3PO_4 (pH 0.7). The samples started fully reduced and were first oxidized (dotted lines) and then reduced (solid lines). The 1st cycle is shown in black, the 11th cycle in red and the 21st cycle in blue. λ_{max} for the reduced species grows in at 362 nm and λ_{max} for the oxidized form is at 443 nm.

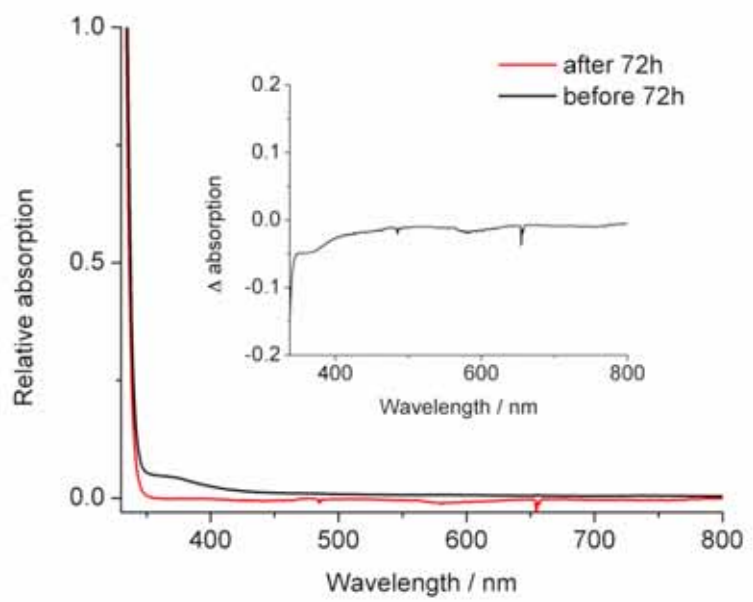

Figure S15. A 0.5 M solution of hydroquinone sulfonate in 1.8 M H_3PO_4 (pH 0.7) before (black line) and after (red line) 72 hours storage in the dark. The inset shows the difference spectrum, where the "before 72 h" graph has been subtracted from the "after 72 h" graph. The difference between the two spectra suggests that spontaneous oxidation of the colorless hydroquinone sulfonate to the red benzoquinone does not occur under these conditions (Δ absorption in the inset is negative, implying a decrease in colored oxidized moieties in the sample after 72 hours storage). By comparison with Figure S7, this suggests that exclusion of light is essential if the reduced hydroquinone is to be stored under aerobic conditions.

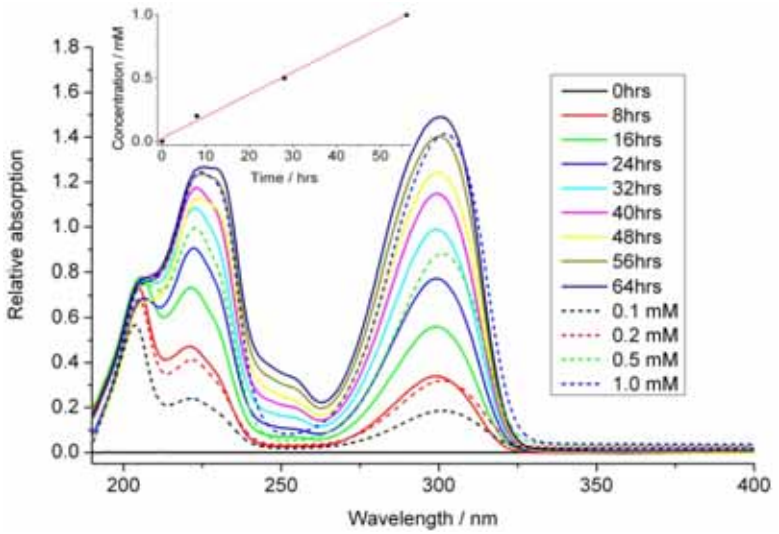

Figure S16. Determination of the rate at which hydroquinone sulfonate crosses the Nafion membrane. Calibration spectra at 0.1, 0.2, 0.5 and 1.0 mM hydroquinone sulfonate in 1.8 M H_3PO_4 (pH 0.7) are shown as dashed lines. For time-dependent crossing assays, a 0.5 M solution of hydroquinone sulfonate in 1.8 M H_3PO_4 (pH 0.7) was placed in one compartment of an H-cell fitted with a Nafion 118 membrane. The second compartment was filled with 1.8 M H_3PO_4 (pH 0.7) and an external fibre optic UV/vis probe was placed in it. Both compartments were stirred and kept in the dark under air. UV/vis spectra were recorded every 60 minutes for 72 hours. By comparison of the calibration and time-dependent data, the rate of crossing was determined to be 2.7 x 10^{-6} mol h^{-1}. The insert shows the concentration of quinone thus determined to be in the second compartment versus time: the linear fit shows that the rate of crossing is also linear.

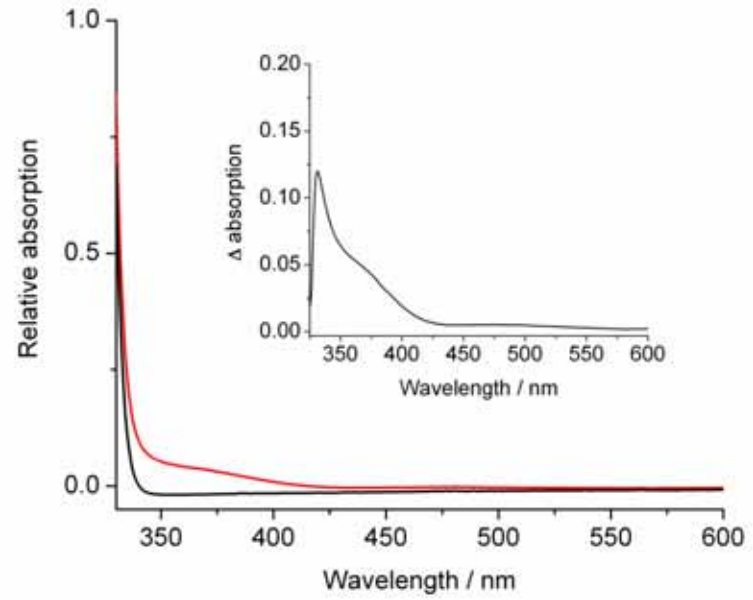

Figure S17. UV-vis Spectra of a 20 mM hydroquinone sulfonate solution in 1.8 M H_3PO_4 (pH 0.7) before (black solid line), and after one full oxidation/reduction cycle (red solid line). The inset shows the difference spectrum, where the "before cyclisation" graph has been subtracted from the "after cyclisation" graph. The difference between the two spectra at 330 nm implies that around 7% oxidized species remain in solution (by comparison with Figures S13a and S14).

References

S1. Hamann, C. H.; Hamnett, A.; Vielstich, W. *Electrochemistry* (2nd. Edition). Wiley-VCH, Weinheim.

S2. Symes, M. D.; Cronin, L. *Nature Chem.* **2013**, *5*, 403.

S3. Erdtman, H.; Högberg, H.-E. *Tetrahedron* **1979**, *35*, 535.